Less is more: Experiments with an individual atomic particle at rest in free space

Hans Dehmelt
Department of Physics, FM-15, University of Washington, Seattle, Washington 98195

(Received 3 October 1989; accepted for publication 16 October 1989)

This article surveys experiments with individual closely confined atomic particles since their beginning in 1973. Such experiments have improved information on the size of an elementary particle on the same level as a quark, the electron, by at least three orders of magnitude. Their extension to the optical region promises atomic clocks of a reproducibility improved up to 100 000 times. The most important of the techniques developed for continuously detecting, cooling, and spin-state analyzing a permanently confined individual electron are described in some detail. The electron, trapped in ultrahigh vacuum at liquid helium temperature, is profitably viewed as a man-made atom, geonium.

I. INTRODUCTION AND SURVEY OF EXPERIMENTS

The history of trapped ion spectroscopy experiments is touched upon in earlier articles.[1–5] Suffice it to say here that it took 17 years of work before in 1973 an individual electron[6] was quasipermanently confined in ultrahigh vacuum in a Penning trap. The close confinement at a point where the electric trapping field vanishes provides a fair approximation of the ideal *experimental* case formulated earlier[1]: an isolated atomic particle at rest in free space. Work was extended to a positron, an antimatter particle, in 1981.[7] In 1984, the same positron was literally observed continuously for 3 months.[8] It was seen to remain during the whole time within a small cylinder in the trap center, about 30 μm in diameter and 60 μm long. There can be little doubt about the identity of this positron as it had practically no chance for trading places with a passing twin. The trap (see Fig. 1) employed a magnetic field of up to 5 T, and an electric axial potential well 5 eV deep. Continuous detection of the electron relied on its axial oscillation in this well, which produced an rf signal (see Fig. 2) that was picked up with a radio receiver. The electron in the trap may be viewed as a pseudo-atom, "geonium,"[9] an atom synthesized for the precision measurement of the g factor. I chose this name also to (a) emphasize the system as it *is*, namely, an electron bound to a magnet and a charged electrode structure affixed to the *Earth*, for once postponing simplifying abstractions, and (b) hint at its distant kinship to Lemaître's "world-atom."[5] The energy levels[10] of the metastable geonium atom are shown in Fig. 3. At a temperature of 4 K preferential occupation of the lowest quantum level $n = 0$ of the cyclotron motion in the trap for periods of about 5 s was demonstrated in 1978 by means of a new quantum state monitor for n, and for the spin quantum number m: the "continuous" Stern–Gerlach effect[5,11] invented in 1973. This effect is the basis of a millionfold amplifier, the first device to perform and *repeat* a quantum measurement on the same individual atomic particle, as often as one pleases. As such, it is the most crucial component in the geonium experiments.

At an ambient temperature of 0 K the electron would within seconds drop into and then permanently remain in the lowest quantum states of cyclotron and axial motions. However, the energy of the metastable low-frequency magnetron motion decreases with radius, which explains its tendency, albeit very slowly, of propelling the electron into the ring electrode of the trap. Accordingly, after injection, radial centering of the electron in the trap is far from spontaneous but requires special ingenuity. Centering was achieved by rf sideband cooling[12] in 1976 (see Fig. 4) in the first such spin and cyclotron resonance experiments.[9] This cooling process is similar to the well-known "optical pumping"[13] of closely spaced atomic sublevels, which suggested already in the 1970 work[4,14] on atomlike electron clouds in a Penning trap that the closely spaced vibrational

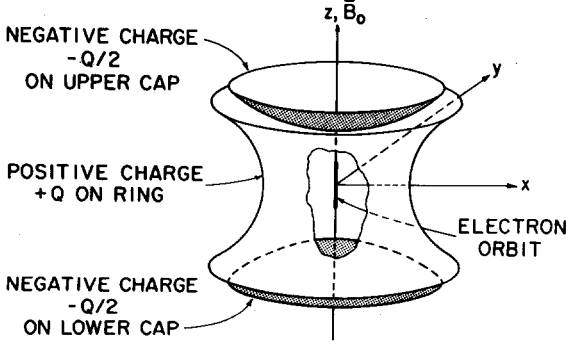

Fig. 1. Penning trap. The simplest motion of an electron in the trap is along its symmetry axis, along a magnetic field line. Each time it comes too close to one of the negatively charged caps it turns around. The resulting harmonic oscillation took place at 60 MHz in our trap. From Ref. 2.

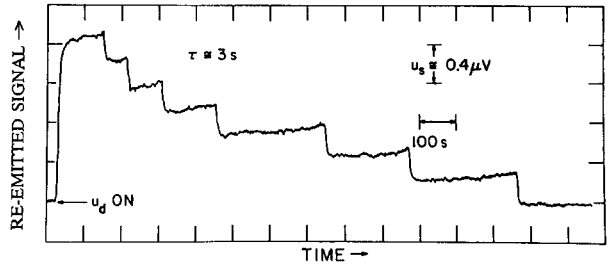

Fig. 2. An rf signal produced by a trapped electron. When the electron is driven by an axial rf field, it emits a 60-MHz signal, which was picked up by a radio receiver. The signal shown was for a very strong drive and an initially injected bunch of seven electrons. One electron after the other was randomly "boiled" out of the trap until finally only a single one was left. By somewhat reducing the drive this last electron could be observed indefinitely. From Ref. 6.

© 1989 American Association of Physics Teachers

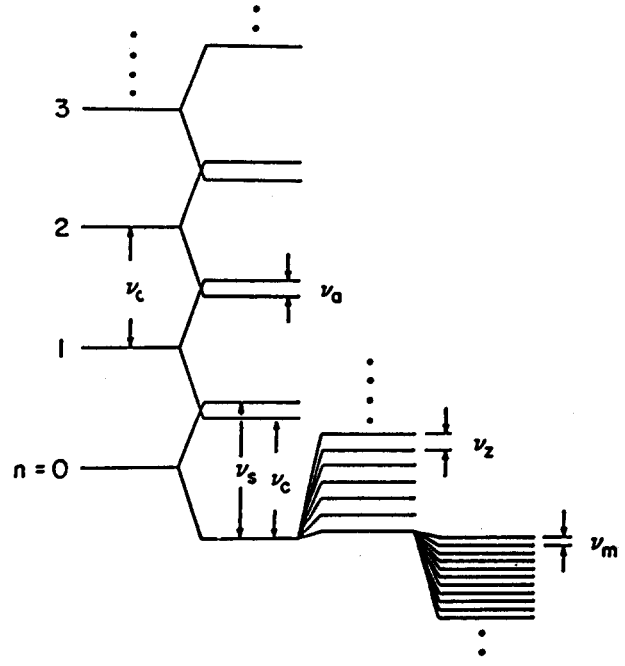

Fig. 3. Energy levels of geonium. From Ref. 10.

levels in the trap might be repopulated and cooled by analogous techniques. It provides a good example why the concept of the geonium *atom* is very useful. In this atom the gyromagnetic ratios $g = 2\nu_s/\nu_c$ for electron and positron were eventually measured[15] to 4 parts in 10^{12} in 1987,

$$\nu_s/\nu_c = 1.001\ 159\ 652\ 188(4).$$

For the theoretical Dirac point electron due to QED shifts not $g = 2$ but the corresponding quantity

$$\tfrac{1}{2} g^{\text{point}} = 1.001\ 159\ 652\ 133(29)$$

has been found.[16] The experimental value was 30 000 times more accurate for the positron than earlier work employ-

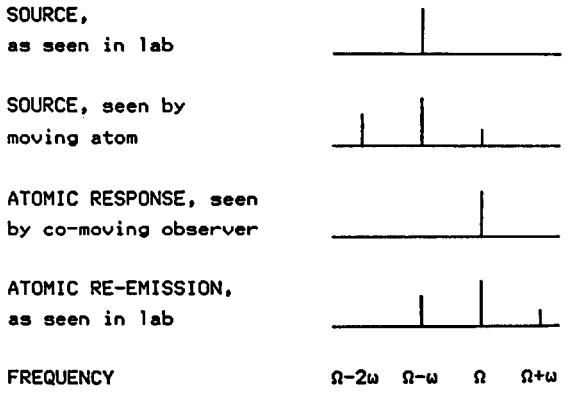

Fig. 4. Sideband cooling of a trapped ion. In the example shown the ion is irradiated by a monochromatic plane electromagnetic wave. Due to the Doppler effect the source signal seen by the ion oscillating in the trap at ω shows sidebands spaced at ω. By proper tuning of the source, the upper sideband is made to coincide with an internal frequency Ω of the ion. The ion is thereby excited. The signal reemitted by the ion is again split by the Doppler effect, but has an average frequency of $\approx\Omega$. In this process a source photon of energy $\hbar(\Omega - \omega)$ is transformed into a reemitted one of energy $\approx\hbar\Omega$ by borrowing $\hbar\omega$ from the oscillatory motion, which is thereby cooled. From Ref. 4.

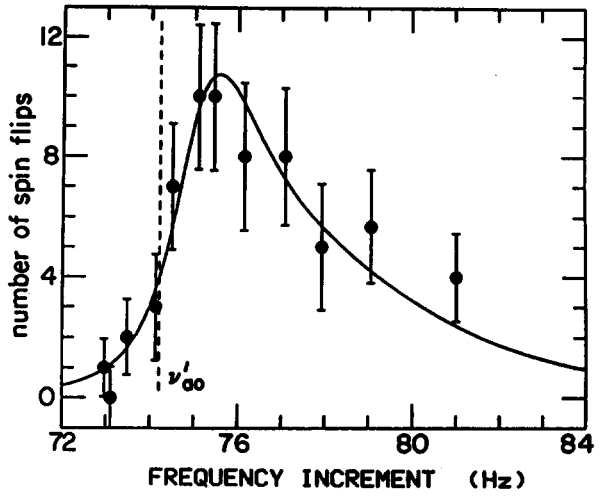

Fig. 5. Electron spin resonance in geonium near 141 GHz. From Ref. 15.

ing other techniques.[3] To this end, spin and cyclotron resonances (see Fig. 5) at ν_s, ν_c were detected via counting by means of the "continuous" Stern–Gerlach effect jumps[5,9,11] (compare Fig. 6) in the m, n quantum numbers induced by suitable rf excitation in resonance with the respective transitions. This new Stern–Gerlach-type effect uses a weak auxiliary magnetic bottle (see Fig. 7). It causes the axial motion orbits for spin ↑ and ↓ to differ measurably in their frequencies, $\nu_z(\uparrow) - \nu_z(\downarrow) \simeq 1$ Hz, at $\nu_z \approx 60$ MHz.

These g measurements severely test the fundamental theory of quantum electrodynamics and the mirror symmetry of e^- and e^+. The value found for the g factor[15] after removal of QED shifts,[16]

$$g = 2.\ 000\ 000\ 000\ 110(60)$$

is by 6 parts in 10^{11} larger than exactly 2, Dirac's value for his theoretical point electron of radius $R = 0$. Taking this at face value, perhaps it is then no great surprise when the true value R is a bit larger than zero too. A plot (see Fig. 8) of the known g factors and rms radii of the near-Dirac particles electron, proton, triton, and ^{3}He then suggests a new experimental value[4,5] for the electron radius,

$$R \approx 10^{-20}\ \text{cm},$$

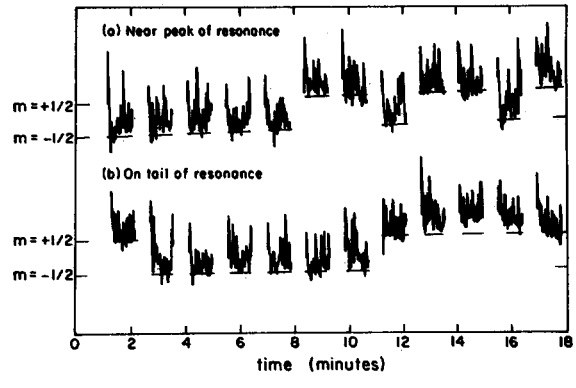

Fig. 6. Jumps in the spin quantum number m for tuning of the excitation (a) on the resonance and (b) on tail of resonance. From Ref. 8.

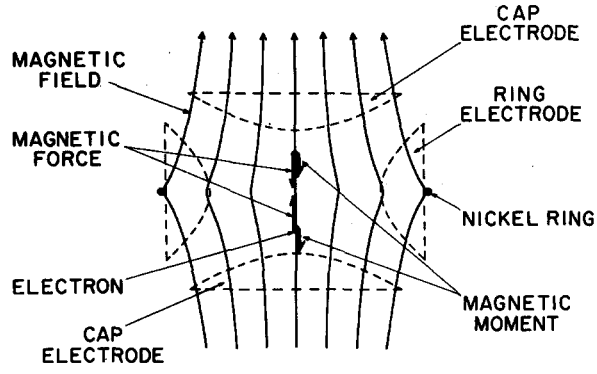

Fig. 7. Weak magnetic bottle for continuous Stern–Gerlach effect. The electron forms a 1-μm-long wave packet, 30 nm in diameter, which oscillates undistorted in the axial electric potential well. The inhomogeneous field of the auxiliary magnetic bottle produces a minute spin-dependent restoring force that causes the axial frequency ν_z for spin ↑ and ↓ to differ by a small but detectable value. From Ref. 2.

which is in agreement with a value from the simplest theoretical model,[17] and 10 000 times smaller than the currently accepted upper limit. Nevertheless, Salam and others[17,18] have proposed that the electron is a composite particle, as are (here I extrapolate[19]) its constituents and their constituents in turn *ad infinitum*. Accordingly, the physical electron and the quarks have extended structure, and are free from point singularities. In quantum field theories the electron is treated as a mathematical point particle. Renormalizing away the artificially infinite mass introduced hereby to the empirical value is revealed as a convenient summary means to handle (or hide) the true extended structure of these particles.

In different laboratories the geonium experiments have been widely extended,[4,20–22] in particular to similar work with an individual proton[23] as well as individual Ba^+, Mg^+, and Hg^+ ions (and soon even an antiproton[24]) in Paul rf and Penning traps. The rf traps[1,2] also use the geometry of Fig. 1 but employ only an electric rf field. I enjoyed a

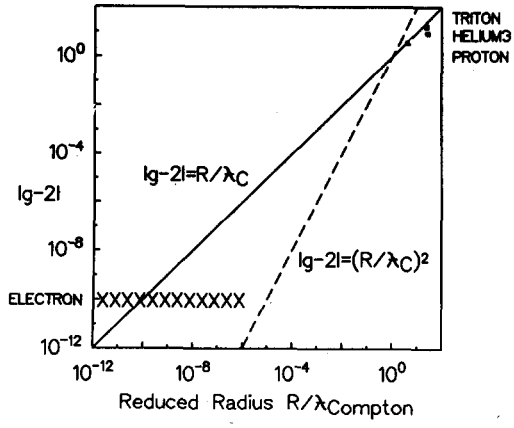

Fig. 8. Plot of $|g-2|$ values, corrected for radiative shift, versus reduced rms radius R/λ for near-Dirac particles. The straight line $|g-2| = R/\lambda$ provides a surprisingly good fit to the data points for proton, triton, and ^{3}He, and may be used to obtain a radius for the electron from our measured g factor. The data are much less well fitted by the relation $|g-2| = (R/\lambda)^2$ which is shown for comparison.

brief spell of euphoria in Seattle, when crucial estimates[20] I had made and published in 1973 for a miniature rf trap with only 0.1-mm cap–cap separation showed that it should be possible to do ultrahigh resolution uv-laser spectroscopy on a localized, refrigerated metastable *single* Tl^+ ion with a resolution equal to the natural linewidth of about 1 Hz and free from all undesirable shifts. One of the two agencies then funding my laboratory was less impressed: They terminated their long-standing support, alleging I was *non compos mentis*. This opinion was not shared by the Humboldt Foundation, which awarded me one of its prizes and by G. zu Putlitz, who invited me to work in his Institut in Heidelberg. The invitation enabled me to build the first prototype miniature rf trap tube (0.2-mm cap–cap separation) and initiate, analyze, and guide to completion the first such single ion spectroscopy experiments[25,26]: As a warm-up exercise for future high-resolution work, the sideband cooling previously demonstrated on an electron was shown to work at optical frequencies, and an individual trapped barium ion was made visible to the eye by illuminating it with laser beams. The ion appears in a microscope as a blue dot about 2 μm in diameter, and was first photographed[26] in 1979 in Heidelberg. *Color* photographs (see Fig. 9) have later been taken in Seattle[4,27,28] using merely an inverted objective from a 35-mm camera, and are reproduced in Refs. 4 and 27. Also, Bohr's quantum jumps[21,22,29] between electronic levels of individual Ba^+ and Hg^+ ions (or charged atoms) were demonstrated in 1986.

Laser resonance fluorescence is an atomic state monitor; it can tell (see Fig. 10) if the barium ion is in its ground S or metastable D state, similarly as the continuous Stern–Gerlach effect can distinguish the two spin states. This state monitor is useful as a millionfold amplifier for the detection of very sharp and therefore slow optical transitions in a similar fashion as in the detection of the spin resonance in geonium, namely, by *counting* quantum jumps. It is this scheme which makes high-resolution spectroscopy on an individual atom practical. Making use of it a cold $(^{204}Tl)^+$ ion in a Paul trap is now available in principle as a shift-free *passive* resonator-type optical frequency standard with Q or quality factor $> 10^{17}$ and the same or better reproducibility for unlimited periods.[30] This is 10 000 times better than the > 3-year reproducibility of the best current atomic clocks and frequency standards, 1 part in 10^{13}, but untested as yet.

Current technical laser imperfections limit the best published *demonstrated* spectral resolution at 10^{15} Hz to 3.4 kHz or 3 parts in 10^{12}, for a Hg^+ ion.[31] As quoted in *Physics Today*, September 1989, the same group has orally reported further 20-fold improvement at meetings. An optical spectrum for a Ba^+ ion[32] is shown in Fig. 11. For Hg^+ also frequent zero-point confinement[20] in two dimensions[33,34] by sideband cooling has been reported. Science progresses through advances in instrumentation, recall Galileo's telescope and Lawrence's cyclotron, and a 10 000 times better clock *is* an advance in instrumentation! To illustrate, impressive *short-term* stabilities as high as $\approx 10^{-15}$ for about an hour are realized with today's microwave atomic frequency standards, but line Q's do not exceed 10^{10}. Perhaps it is then no great surprise that reproducibilities are no better than quoted above: The atomic resonance has already been split 100 000-fold! By contrast, in the case of $(^{204}Tl)^+$, the reproducibility projected is just the unsplit natural linewidth. The quoted reproducibility[30] of 1 part in 10^{17}, unlimited in time, translates over an observation peri-

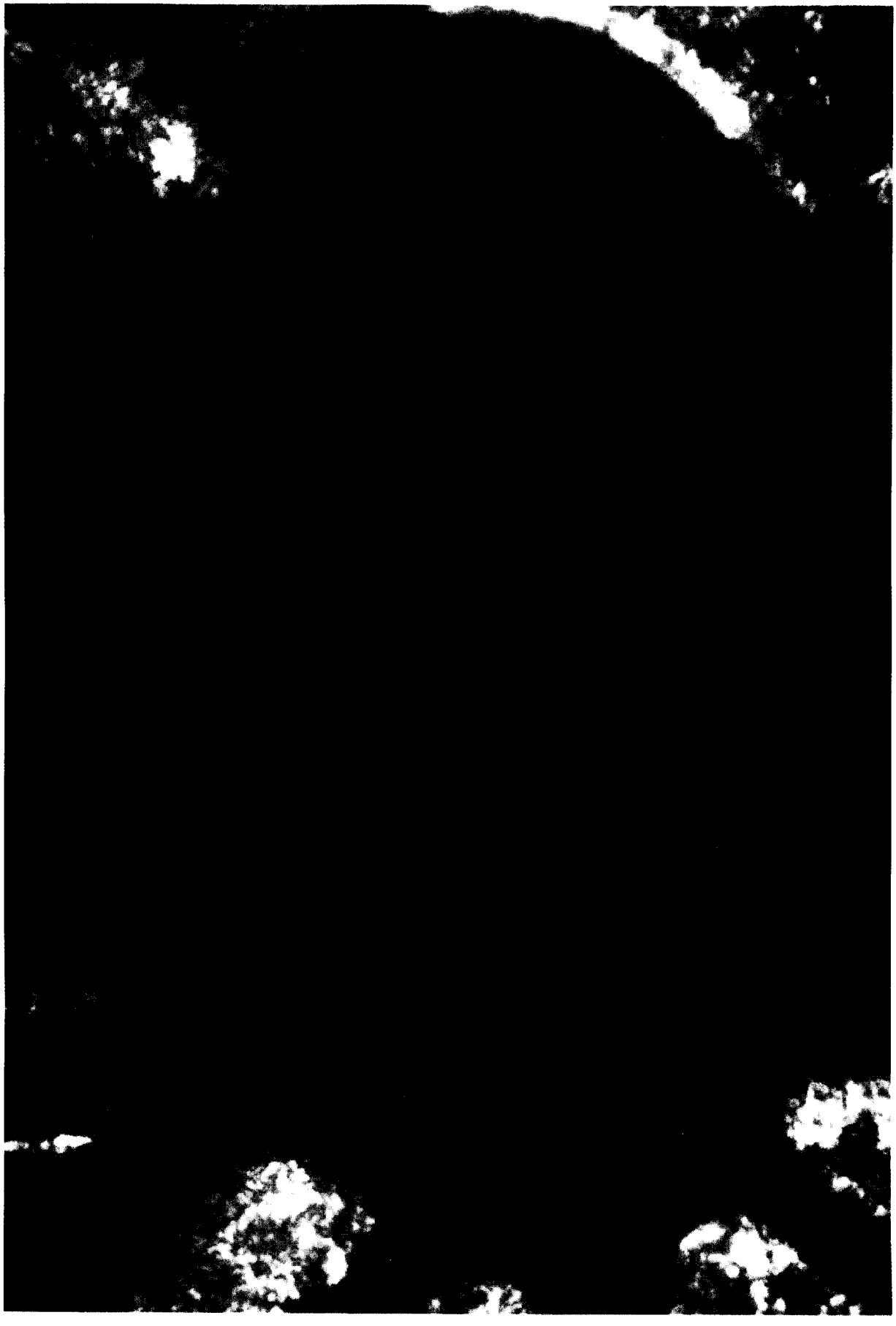

Fig. 9. Photograph of individual bluish-white barium ion Astrid. Stray light from the lasers focused on the ion also illuminates the 0.7-mm i.d. ring electrode of the tiny rf trap. From Refs. 4 and 27.

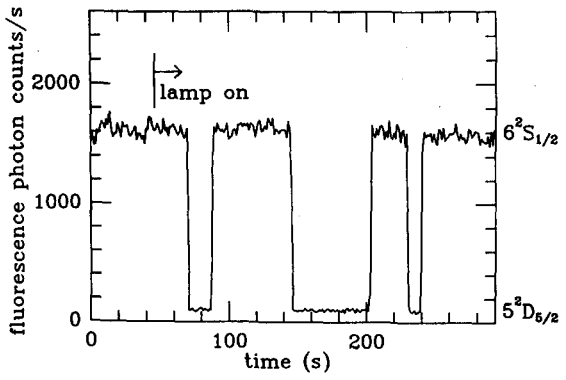

Fig. 10. "Shelving" the Ba^+ optical electron in the metastable D level. Illuminating the ion with a laser tuned close to its resonance line produces strong resonance fluorescence and an easily detectable photon count of 1600 photons/s. When later an auxiliary, weak Ba^+ spectral lamp is turned on, the ion is randomly transported into the metastable $D_{5/2}$ level of 30-s lifetime and becomes invisible. After dwelling in this shelving level for 30 s on the average, it drops down to the S ground state spontaneously and becomes visible again. This cycle then repeats randomly. According to the Zeno no-go theorem, no quantum jumps should occur under continuous observation, see Sec. V B. From Ref. 29.

od of 3 years or $\approx 10^8$ s into a sensitivity sufficient for detecting a slow continuous frequency drift as small as 1 part in 10^{25}/s. Such sensitivity should allow a meaningful search for sequels of the about 1 part in 10^{18}/s Hubble expansion of the universe, which are detectable in the laboratory. Also worthy of contemplation are the philosophical implications of the now emerging realization that all man-made clocks in the known part of the universe may potentially be locked to an ultrastable internal motion of the *same* permanently confined (charged) atom.[20]

In the following sections I will discuss in much more detail some crucial elements of the geonium experiments.

II. PENNING TRAP

The 1973 monoelectron oscillator experiment used a centimeter-sized trap, which employed a strong, homogeneous magnetic and a weak, quadrupole electric field with the saddle point in the trap center. This device (see Fig. 1), which I demonstrated[1,2,4] in 1959 and named a Penning trap, is related to the magnetron invented by Hull in 1921. The latter is now most widely used to generate kilowatt radiation via oscillatory motions of large electron clouds in microwave ovens in the kitchen. Thus it is perhaps no wonder that, with some effort, it is possible to detect even the radiation given off by a single oscillating electron. The trap is related also to Lawrence's 1932 cyclotron, the progenitor of most current atom smashers. Most immediately it is derived from a gas discharge tube demonstrated by Penning in 1936. The device is well suited for measurements of spin and cyclotron frequencies because the perturbations caused by the weak electric field, which vanishes in the center of the trap, are very small and well understood.

An electron moving along a magnetic field line experiences only an electric force. In accordance with the applied potential

$$\phi = A(x^2 + y^2 - 2z^2), \quad A > 0, \tag{1}$$

on the trap axis this force has only a z component, $e\,\partial\phi/\partial z = -4eAz$. In the axial parabolic potential well the electron experiences a restoring force with a force constant $k = 4eA$ and oscillates with a frequency ω_z,

$$\omega_z^2 = 4eA/m_e. \tag{2}$$

The electric quadrupole field only slightly perturbs the circular cyclotron motion and shifts its frequency down from $\omega_c = eB_0/m_e c$ a little by δ_e to ω_c'. In order to describe[1-3] the motion of an electron in the midplane of the trap, or for $z = 0$, we use Newton's second law and assume first only circular orbits, as in the zero E-field case,

$$-evB_0/c - eE = -m_e v^2/r, \tag{3}$$

with $r^2 = x^2 + y^2$. The electric force is only radial here and it holds,

$$E = -\frac{\partial\phi}{\partial r} = -2Ar = -\frac{m_e\omega_z^2 r}{2e}. \tag{4}$$

Using $v = r\omega$, the above expression for ω_c, and with (1) and (4), Eq. (3) takes on the form of a quadratic equation for ω,

$$\omega^2 - \omega_c\omega = -\omega_z^2/2. \tag{5}$$

One of its two solutions is $\omega = \omega_c'$, the shifted cyclotron frequency. Going with this into (5) immediately gives the very useful expression for the difference $\omega_c - \omega_c' = \delta_e$, the electric field shift of the cyclotron frequency,

$$\delta_e = \omega_z^2/2\omega_c', \tag{6}$$

in terms of the experimentally determined frequencies ω_z, ω_c'. Next we see by substitution that

$$\omega = \omega_m = \delta_e \tag{7}$$

is the other root of the quadratic equation (5). The frequency ω_m is that of the very slow drift or "magnetron" motion in the trap.

The trap used in the Seattle experiments[8-10] had an axial cap–cap separation $2Z_0 = 0.67$ cm and a radius $R_0 = \sqrt{2}Z_0$. For a potential $V_0 \approx 10$ V applied between ring and connected cap electrodes an axial oscillation frequency

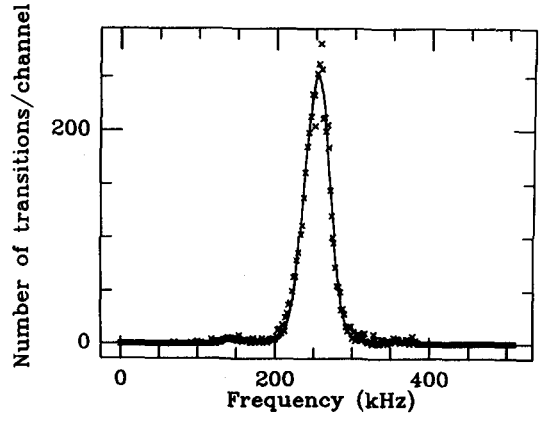

Fig. 11. Spectrum of forbidden optical transition in Ba^+ recorded by the shelving technique. As the exciting laser is stepped through the resonance near 2×10^{14} Hz and of 0.005-Hz natural width, the ion jumps rapidly between ground and metastable states. These jumps are made visible, as illustrated in Fig. 10, and their count in a fixed time interval is then plotted on the vertical axis by computer. The observed linewidth of 35 kHz is mostly due to the laser and to a much lesser degree due to as yet unshielded stray 60-Hz magnetic fields from the mains, which Zeeman shifts the atomic transition. From Ref. 32.

$\omega_z \approx 60$ MHz was measured. This electric field resulted in a magnetron frequency ω_m and a cyclotron frequency shift $\delta_e \approx \omega_m$ of only $\approx 2\pi \times 13$ kHz for a cyclotron frequency $\omega_c = 2\pi \times 141$ GHz. Figure 3 shows that the magnetron motion is metastable. If one couples a resonant circuit to it, an electron released in the trap center can be made to give up its predominantly potential energy to the circuit and to spiral outward into the ring electrode. This is the process used in the magnetron tubes of microwave ovens.

Recent models of the trap were enclosed in an evacuated, sealed-off copper envelope that was submerged in liquid helium. A built-in cryopumping element reduced the residual (He) gas density to an estimated 1 atom/cm.[3] In order to realize the extremely narrow axial resonances crucial for the spin resonance experiment the simple structure shown in Fig. 1 had to be supplemented by a symmetric pair of compensation ring electrodes[10,11] mounted in the gap between cap and ring electrode. This greatly reduced the anharmonicity of the axial potential and made it possible to attain the high spectral resolution in the axial resonance necessary for the continuous Stern–Gerlach effect.

III. TRAPPED ELECTRON–RESONANT CIRCUIT INTERACTION

A. Signal induced in circuit—electron cooled

Before one can perform any experiments on the electron, one must obviously establish a line of communication with it. The axial oscillation of the trapped particle has proven itself as most effective for this purpose since it falls in the radio/television frequency range where the highly developed technology easily lends itself to the detection of threshold signals. To bring out the essential points, we analyze[2,35] the ion–circuit interaction for an elastically bound ion of charge e and mass M which is placed inside a parallel plate capacitor C forming part of a resonant LCR_S circuit (see Fig. 12). We expect that an ion oscillation of energy

$$W_I = M\langle v^2 \rangle \tag{8}$$

will excite the LCR_S circuit to a slowly declining energy W_T after transients in the damped circuit have quickly died out in its characteristic decay time τ_{TB}. Here, v is the ion velocity and the averages are over one period. The slowly varying value W_T is determined by the requirement that the energy input from the ion $P = -\langle dW_I/dt \rangle$ must balance the loss from the LC circuit into R_S,

$$P = W_T/\tau_{TB} = W_I/\tau_{IT}. \tag{9}$$

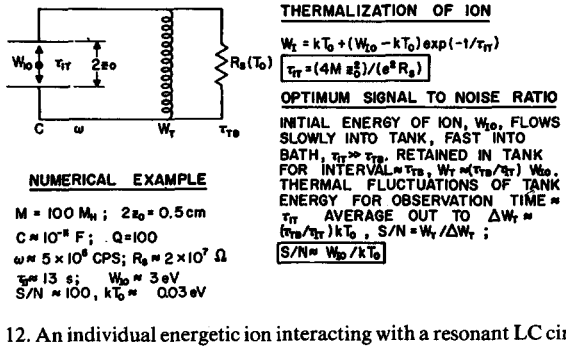

Fig. 12. An individual energetic ion interacting with a resonant LC circuit induces a signal in the circuit and is damped and cooled by the interaction. From Refs. 2 and 35.

Here, we have introduced the decay time τ_{IT} of the ion energy due to the coupling to the LCR_S-tuned circuit. In more detail, for exact resonance between ion and circuit oscillations, the electric rf field between the capacitor plates extracts energy from the ion oscillation according to

$$P = e\langle vE \rangle, \quad P^2 = e^2\langle v^2 \rangle \langle E^2 \rangle. \tag{10}$$

We have used $v = GE$, $G = \text{const}$ here. The field E inside the flat capacitor C with plate spacing $a = 2Z_0$ and the energy W_T stored in the LCR_S circuit are related by

$$W_T = Ca^2\langle E^2 \rangle. \tag{11}$$

Using first (8)–(11) to eliminate all variables we arrive at a relation between the decay times:

$$\tau_{IT} = Ca^2M/e^2\tau_{TB}. \tag{12}$$

Making use of $\tau_{TB} = \mathrm{R}_S\mathrm{C}$, R_S being the shunt resistance of the damped LCR_S circuit, we find the desired expression of the ion damping time in apparatus parameters

$$\tau_{IT} = a^2M/e^2\mathrm{R}_S. \tag{13}$$

Substituting the cap–cap separation $2Z_0$ for a, these results, as listed in Fig. 12, may be applied to an ion confined in a hyperbolic trap in fair approximation.

In Fig. 12 we have also allowed for the thermal energy kT_0 that according to the equipartition theorem the ion oscillator acquires via the thermal noise voltage that at temperature T_0 appears across the LCR_S circuit. The numerical example in Fig. 12 shows that, even for heavy ions, cooling times of seconds are easily realized, an important result. Since the cooling times listed are many orders of magnitude smaller than via dipole radiation into free space, the damping process may also be viewed as enhanced spontaneous emission.[36] The reasoning leading to Eq. (13) may be extended to an elastically bound electron or even a two-quantum level system, an atom, in a resonant cavity $> \lambda$. The opposite case, in which an atomic radiator is shielded by a nonresonant enclosure from coupling to standing-wave oscillators of similar frequency in the infinitely large free-space "cavity" is also of great interest. Here, a tenfold increase in the lifetime against spontaneous emission for the cyclotron motion of the electron in geonium due to the presence of the trap cavity has been demonstrated.[4,8] Related shifts in ω_c are no serious threats to precision g-factor measurements because they can be nulled[4] by proper fine-tuning of the magnetic field and thereby ω_c.

We now turn to the detection of the coherent excitation at ω of the LCR_S tank circuit by an energetic ion that is quickly dissipated into the heat bath in a characteristic time $\tau_{TB} \ll \tau_{IT}$. For the initial signal in the tank circuit, we have from (9)

$$W_{T0} = (\tau_{TB}/\tau_{IT})\, W_{I0}. \tag{14}$$

If one chooses the detection bandwidth so wide that it passes the full width $\omega/Q = 1/\tau_{TB}$ of the noise spectrum of the damped LCR_S circuit, then in the example of Fig. 12 the ratio of signal energy to noise energy would be W_{T0}/kT_0 or only about 0.002. However, by decreasing the observation bandwidth to, say, $\Delta\omega \approx 1/\tau_{IT}$, which necessitates increasing the observation time to $\tau_{IT} \approx 13$ s, the noise energy registered in the narrow observation channel drops to $(\tau_{TB}/\tau_{IT})kT_0$. This raises the signal-to-noise power ratio S/N available from an individual ion to a quite practical value

$$\mathrm{S/N} = W_{I0}/kT_0 \approx 100. \tag{15}$$

B. Continuous detection of electron oscillation

The essential piece of apparatus that makes the nearly 100 000-fold reduction of the bandwidth possible is a phase-sensitive detector in conjunction with a continuous coherent excitation of the ion oscillation. The 60-MHz front end of the detection circuit actually used[10] in the trapped electron or geonium experiments is shown in Fig. 13 in simplified form. The electrostatic trapping potential is produced by a block of stable standard cells providing 9.2 V. The axial oscillation is continuously excited by applying a small drive voltage at $\nu_z = 60$ MHz nominally to one end cap. In an alternative picture to that used in the preceding section, the oscillating electron behaves similar to another harmonic oscillator, a series resonant circuit[6,14]: On resonance a large current flows through this equivalent resonant circuit and the connected physical parallel resonant LCR circuit formed by a low-loss coil and the cap-to-ring capacity and thereby excites the latter. Here, for the case of exact resonance, only the shunt resistance of this LCR circuit is shown in the figure. The 60-MHz signal developed across this shunt resistance is then amplified about a millionfold and fed into the phase-sensitive detector, shown as a crossed circle. The other input of the detector is a reference signal, which is provided by the drive generator at ν_{zd}, and whose phase can be adjusted. With the lead to the integrator cut in Fig. 13, the output signal of the detector may be displayed on a chart recorder as the resonance frequency ν_z of the electron is slowly swept through resonance with the drive by slightly varying the trapping potential (see Fig. 14). By proper adjustment of the phase of the reference signal, both absorption and dispersion modes of the axial resonance of the electron may be displayed. The reduction of noise in the center of resonance is real: The equivalent series resonant LC circuit for the electron with a quality factor $Q \approx \infty$ effectively short circuits[37] the noise producing resistance at $T = 4$ K (compare Fig. 13).

While we have shown above that the expected electron signal is larger than the thermal noise background, the experiment is still plagued by more mundane interference, as in our scheme the continuous electron signal is produced in the presence of a much larger drive voltage at the same frequency. The small cap–cap capacitance causes a large background signal to appear across the LCR circuit even in

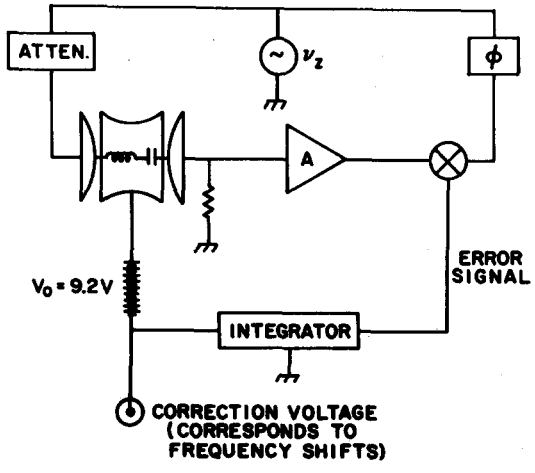

Fig. 13. Detection circuit for the axial resonance at ν_z. The elastically bound electron oscillator acts effectively like an LC resonant circuit oscillator. The device also locks the electron frequency to that of the very stable drive generator. From Ref. 10.

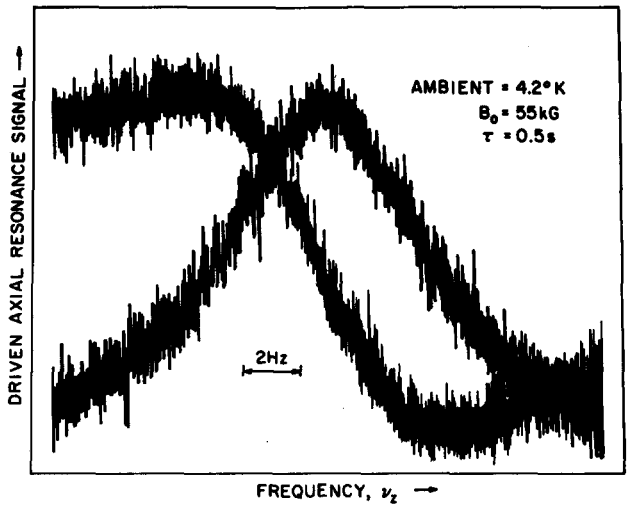

Fig. 14. Plots of driven axial resonance amplitudes versus electron eigenfrequency ν_z. The latter is slowly swept by varying the depth of the confining potential well. The graph shows the absorption mode and also the S-shaped dispersion mode, for which the zero is raised. Note the about 1 part in 10^7 width of the resonance! From Ref. 10.

the *absence* of an electron, which moreover is modulated by microphonics. This problem was solved by a scheme adapted from NMR techniques. We will discuss it because it provided an early example of the importance of sideband excitation schemes[6,14] in trapped ion spectroscopy. The essence of the scheme is that it allows excitation of the axial oscillation at a frequency different from that at which it is detected. We recall that weak frequency modulation at ω_M of an rf signal at ω_z produces a couple of weak sidebands at $\omega_z \pm \omega_M$ [compare Fig. 4 and Eq. (17) below]. The same is true when the depth of the axial potential well is modulated at ω_M. It now turns out that the same frequency-modulated axial oscillation of the electron may be excited in three ways: weakly when the drive at ω_d is tuned to one of the sidebands and strongly, when tuned to the carrier. An easy way to see this without analyzing the frequency-modulated harmonic oscillator is the following. The excitation depends only on the relative tuning of the drive and oscillator in good approximation. Thus modulating the oscillator or the drive (with a phase shifted by π) should produce essentially the same excitation. However, the frequency-modulated drive is again the textbook case mentioned above and obviously excites the electron oscillator of fixed frequency ω_z strongly for a tuning $\omega_d = \omega_z$, and weakly for $\omega_d \pm \omega_M = \omega_z$. (Irrespective of subscripts we use the convention $\omega = 2\pi\nu$ throughout the paper.) In order to use sideband excitation in the experiment, the $\approx$10-V dc potential for the ring is supplemented by a 1-MHz rf potential and the drive is tuned to the sideband at 59 MHz while the carrier at 60 MHz nominally is detected by the electronics. The scheme resembles an atomic fluorescence that occurs at another frequency than the excitation.

IV. CLASSICAL MODEL OF SIDEBAND COOLING

This very important process is another application of sideband excitation. The simple explanation of sideband cooling given in Sec. I relied only on basic quantum concepts and an energy balance. However, an alternative,

purely classical description making use of modulated light pressure exerted by a plane wave

$$E = E_0 \cos(\Omega' t - z/\Lambda), \quad \Lambda\Omega = c, \tag{16}$$

tuned to the lower sideband, has also been given.[38,39] To this end, we consider a positron that is elastically bound to the origin with direction-dependent force constants. It is free to oscillate only along the z axis at ω, $z = z_0 \cos \omega t$, and at Ω in the y direction, with $\Omega \approx \Omega' \gg \omega$. The electric field of the wave points in the y direction and, as seen by the positron, is frequency modulated at ω and has the form

$$E \approx E_0 \cos \Omega' t + (E_0 z_0/2\Lambda)[\sin(\Omega' + \omega)t + \sin(\Omega' - \omega)t] \tag{17}$$

in the limit $z_0/\Lambda \ll 1$. This field has additional spectral components E_+, E_- at $\Omega' + \omega$, $\Omega' - \omega$ (compare Fig. 4), whose amplitudes are $z_0 E_0/2\Lambda$. For the tuning $\Omega' + \omega = \Omega$, the y-motion resonance is excited by the E_+ component. With V the positron velocity, we have for this driven oscillation

$$V = (e z_0 E_0/2 m_e \Gamma \Lambda) \sin \Omega t, \tag{18}$$

where $\Gamma \ll \omega$ is the radiation damping constant for the Ω oscillation. In the magnetic field B of the wave the positron experiences a Lorentz force in the z direction

$$F = eVB/c = (e^2 E_0 B_0 z_0/2 m_e c \Gamma \Lambda) \sin \Omega t \cos \Omega' t, \tag{19}$$

which has a spectral component $F_- = F_{+0} \sin \omega t$, since $\Omega - \Omega' = \omega$. Note that for the tuning $\Omega' = \Omega + \omega$ the corresponding force F_+ has the opposite sign.

These forces *extract /add* power from/to the essentially free and undamped z oscillation of energy

$$W = \tfrac{1}{2} m_e \omega^2 z_0^2 \tag{20}$$

at a rate

$$\left| F_- \frac{dz}{dt} \right| = \left(\frac{e^2 z_0^2 \omega}{4 m_e c \Gamma \Lambda} \right) E_0 B_0 \sin^2 \omega t. \tag{21}$$

In the cooling mode $\Omega' = \Omega - \omega$, this is, after averaging over one period $2\pi/\omega$, equivalent to

$$\frac{dW}{dt} = \frac{-W}{\tau}, \quad \frac{1}{\tau} = \frac{e^2 E_0^2}{4 m_e^2 c \Gamma \Lambda \omega}. \tag{22}$$

In this expression, τ denotes the characteristic time with which sideband cooling proceeds, and we have used $B_0 = E_0$ in cgs units. Equation (22) indicates exponential cooling to zero oscillatory energy.

At an ambient temperature T the thermal background radiation also excites[38] the oscillatory motion at Ω to a velocity V', which randomly varies in amplitude and phase, and for which

$$m_e \langle V'^2 \rangle = kT. \tag{23}$$

In conjunction with the B field of the cooling wave at $\Omega' = \Omega - \omega$ this produces an oscillatory Lorentz force f that randomly *excites* the z oscillation at ω. This sets a limit to the sideband cooling as follows. In the expression for

$$f = (e/c) V' B_0 \cos \Omega' t, \tag{24}$$

we approximate V' by a sequence of short pulses

$$V' = P \sin \Omega t, \tag{25}$$

one immediately following the other, of fixed duration $t_p = 2\pi/\Gamma$ and amplitude $P = \pm P_0$, which randomly switches sign. We make $P^2 = 2\langle V'^2 \rangle$ in order to make the power in V' and the pulse approximation the same. For the pulse duration chosen, the width of the resulting simulated V' noise spectrum centered on Ω is about Γ and thereby approximates the width of the thermal noise band capable of exciting the Ω oscillation. The Lorentz force now also is pulsed and shows a spectral component

$$f_- = -(e/2c) P B_0 \sin \omega t \tag{26}$$

that reflects the pulse structure assumed for V'. Also, it is well known that the amplitude z_0 of a slightly damped harmonic oscillator when excited on resonance by a sinusoidal drive force $f = f_0 \sin \omega t$ initially increases linearly with time t,

$$z_0 = (f_0/2 m_e \omega) t, \tag{27}$$

and decreases linearly when the phase of the drive is reversed. Accordingly, when starting from an initial value 0, the oscillation amplitude z_0 will execute a random walk described by

$$\langle z_0^2 \rangle = (\Gamma/2\pi) t s^2, \tag{28}$$

with a step size corresponding to $t_p = 2\pi/\Gamma$, and $f_0 = -(e/c) P B_0$,

$$s = \pi e P B_0/2 m_e c \omega \Gamma. \tag{29}$$

The average oscillatory energy is

$$\langle W \rangle = \tfrac{1}{2} m_e \omega^2 \langle z_0^2 \rangle, \tag{30}$$

and thus increases linearly with time t,

$$\langle W \rangle = (\pi e^2 P^2 B_0^2/16 m_e c^2 \Gamma) t. \tag{31}$$

In the presence of sideband cooling the increase of $\langle W \rangle$ is described by

$$\frac{d\langle W \rangle}{dt} = \frac{\pi e^2 P^2 B_0^2}{16 m_e c^2 \Gamma} - \frac{\langle W \rangle}{\tau}. \tag{32}$$

This vanishes for $\langle W \rangle = kT_{z\min}$, yielding the relation

$$(\pi e^2 P^2 B_0^2/16 m_e c^2 \Gamma) = kT_{z\min}/\tau. \tag{33}$$

Substituting for P and τ from Eqs. (22) and (25), and with $E_0 = B_0$ we obtain for the minimum temperature of the oscillatory z motion in the trapping well that can be attained when the ambient temperature has the value T

$$T_{z\min} = (\pi/2)(\omega/\Omega) T. \tag{34}$$

With $kT \approx \langle n_y \rangle \hbar\Omega$, $kT_{z\min} \approx \langle n_z \rangle \hbar\omega$, and $\langle n_y \rangle$, $\langle n_z \rangle$ the corresponding average quantum numbers for the respective oscillations, this expression reduces to

$$\langle n_{z\min} \rangle \approx \langle n_y \rangle \gg 1, \tag{35}$$

or in words: Sideband cooling cannot reduce the average quantum number of the cooled motion below that taken on under thermal excitation by the motion used for cooling. In the absence of other causes of heating, this is independent of the width Γ of the y-motion resonance used for cooling, and the intensity of the cooling wave as long as $\Gamma \ll \omega$.

Using a standing Ω' wave[40] with an E-field node at the origin for sideband cooling may be analyzed in a similar fashion. It has some advantages as the carrier and heating associated with it disappear.[34] The latter model is helpful in describing sideband cooling in geonium. The inhomogeneous rf field at $\omega_z \pm \omega_m$ can be viewed as a standing wave, which is equivalent to two waves traveling in the opposite direction. Figure 15 shows the heating and cooling effects when the excitation frequency is first tuned to the lower and then the upper sideband. This 1977 demonstration[10] of sideband cooling at an rf frequency was soon followed by work in the optical region.[4,21,25]

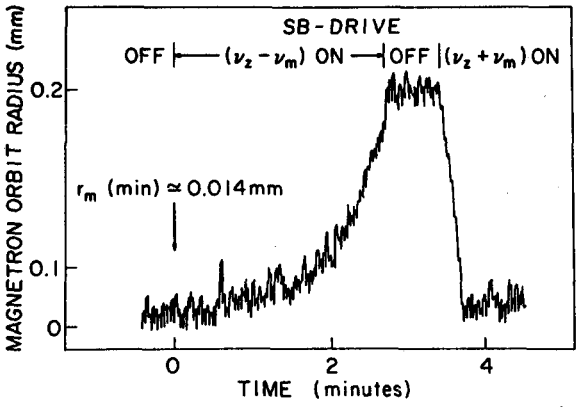

Fig. 15. Sideband "cooling" of the magnetron motion at ν_m. By driving the axial motion not on resonance at ν_z but on the lower sideband at $\nu_z - \nu_m$ it is possible to force the magnetron motion to provide the energy balance $h\nu_z$, and thereby expand the magnetron orbit radius. Conversely, an axial drive at $\nu_z + \nu_m$ shrinks the radius. The roles of upper and lower sidebands are reversed here from the case of a particle in a well where the energy increases with amplitude because the magnetron motion is metastable and the energy of motion *decreases* with radius. From Ref. 10.

V. CONTINUOUS STERN–GERLACH EFFECT

A. Frequency shift proportional to magnetic moment

For the *continuous* version of the effect in geonium the strong inhomogeneous Stern–Gerlach field used for spin-dependent deflection in beam experiments is replaced by a shallow magnetic bottle (see Fig. 7). It is so weak that unlike in atomic beam resonance experiments magnetic resonance spectroscopy may be performed *inside* the inhomogeneous field region with almost negligible line broadening. In the first experiments[9,10] the bottle was produced by three turns of 5-mil nickel wire wound around the ring electrode. The large applied magnetic field $\mathbf{B}_0$ magnetized the wire to saturation and produced a bottle field $\mathbf{b}$, practically independent of $\mathbf{B}_0$. Near the origin, the trap center, its components were, with $\beta \approx 120$ G/cm^2,

$$b_x = -\beta z x,$$
$$b_y = -\beta z y, \tag{36}$$
$$b_z = \beta(z^2 - \tfrac{1}{2}r^2), \quad r^2 = x^2 + y^2,$$

and added to $\mathbf{B}_0$. Expression (36) satisfies Maxwell's equations, which here take the simple form $\operatorname{div}\mathbf{b} = 0$ and $\operatorname{curl}\mathbf{b} = 0$. The success of the scheme was first shown by exciting the cyclotron motion and watching for a shift in the axial frequency ω_z. The quantized energy of the cyclotron motion is given by

$$E_n = (n + \tfrac{1}{2})\hbar\omega_c. \tag{37}$$

By setting

$$-\mu_n B_0 = E_n, \tag{38}$$

one can assign a quantized magnetic moment $\mu_n = -(n + \frac{1}{2})\mu_B$ to the nth cyclotron level. This magnetic moment interacts with the magnetic bottle. On the z axis the difference of the potential energy of the positron at $z = Z_0$ and $z = 0$, or the total depth D of the axial confining well, is then given by

$$D = D_e + D_m, \quad D_m = -\mu_n \beta Z_0^2, \tag{39}$$

where $D_e = 5$ eV is the electrostatic part of the well depth, and $D_m \approx 0.2\ (n + \frac{1}{2})$ μeV is the magnetic "Stern–Gerlach" contribution. Since for a confining well with fixed Z_0 the relation between oscillation frequency, force constant, well depth

$$\omega_z^2 \propto k \propto D \tag{40}$$

holds, and $D_m \ll D_e$, we have for the shift associated with the nth cyclotron state

$$\delta\omega_z \approx \tfrac{1}{2}(D_m/D_e)\omega_z = (n + \tfrac{1}{2})\delta,$$
$$\delta = 2\mu_B\beta/m_e\omega_z \approx 2\pi \times 1 \text{ Hz}, \tag{41}$$

with $\mu_B = e\hbar/2m_e c$ the Bohr magneton and m_e the electron mass. In earlier experiments we had established that our weak millimeter wave source was strong enough to produce detectable heating effects in clouds of ≈ 1000 electrons suggesting average n values > 100. Thus cyclotron resonance was easily detected with the new much more sensitive continuous Stern–Gerlach effect. In fact, we were able to see the excitation of the n levels by the thermal radiation field at 4 K. Examining Fig. 6, for which $\langle n \rangle \approx 0.23$, one recognizes frequent intervals of an average length of about 5 s for which $m = -\frac{1}{2}$, $n = 0$. This shows that for the spin and also at least for one degree of freedom of the translational electron motion the zero-point energy is frequently attained.

Recognizing that spin and magnetron motions are associated with quantized magnetic moments

$$\mu_m = -2m\mu_B, \quad \mu_q \approx -q(\omega_m/\omega_c)\mu_B, \tag{42}$$

m, q spin, and magnetron quantum numbers, we may extend (41) as follows

$$\delta\omega_z \approx [m + n + \tfrac{1}{2} + (\omega_m/\omega_c)q]\delta. \tag{43}$$

The weak q dependence was sufficient for the demonstration of sideband cooling in Fig. 15.

B. Measurement of frequency shift

By adjusting the phase ϕ of the reference signal in the phase-sensitive detector circuit shown in Fig. 13, one may obtain the S-shaped dispersion signal of Fig. 14, for which the zero-response level has been raised in the graph. One sees that the signal vanishes on exact resonance, and near zero decreases linearly with frequency. Obviously, this signal could serve to detect a small frequency shift of 1 Hz in the axial resonance with good signal/noise ratio. Because of slow drifts in battery voltage for the axial potential well, however, it is experimentally more convenient to lock the resonance frequency of the electron to that of the very stable drive generator. To this end, the phase is set to π plus the value used for the dispersion signal shown in Fig. 14 in order to reverse its sign, and the amplified signal voltage is added to the battery voltage (compare Fig. 13). We see that when, for example, the battery voltage and the electron frequency ν_z have drifted to a value above that for exact resonance with the generator, a negative signal current appears at the output port of the detector. This current charges up a capacitor, the integrator of Fig. 13, to a voltage just large enough to compensate exactly the increase in the battery voltage. The larger the gain of the amplifier in Fig. 13, the more promptly the electron is kept on exact resonance with the generator. On the other hand, when the electron frequency ν_z changes due to a spin flip, the integrating capacitor voltage reflects this and serves as *the* principal frequency shift monitor for the continuous Stern–Gerlach effect. Its analog in the classic Stern–Ger-

lach effect for atomic beams is the glass plate on which the beam of silver atoms was collected.

Before the first spin flip was observed, I briefly worried about a no-go theorem, termed the Zeno paradox, which asserted that "continuous observation freezes the evolution of an otherwise evolving state." The inapplicability of this theorem to the physical world appears to be related to a crucial difference between measurements on atomic systems carried out in the heads of some theoreticians and in the laboratory. As already criticized by Pauli,[5] the latter require time while the former do not. Before the conclusion of a measurement can force the wavefunction to collapse, there is still plenty of time for a strong enough perturbation to modify it, see, e.g., Fig. 10.

VI. TWO-PHOTON SPIN RESONANCE

The most straightforward approach to measuring the spin precession frequency ω_s would seem to be as follows. Induce random up and down jumps between the two spin states $m = -\frac{1}{2}$ and $+\frac{1}{2}$ by irradiating the electron with a millimeter wave whose frequency ω_{sd} is slowly stepped through the resonance at ω_s. Remaining at each step for the same fixed time interval, say 20 min, by constantly monitoring the axial frequency ω_z, count the number of jumps by means of the continuous Stern–Gerlach effect. Then plot the counts versus the frequency of the rf drive used for excitation. Alas, this straightforward approach is far from optimal when $\omega_s \approx \omega_c$. In order to see this, we write

$$\omega_s/\omega_c = 1 + (\omega_s - \omega_c)/\omega_c. \tag{44}$$

The chief cause for measurement error in ω_s, ω_c are random fluctuations of B_0. For an average fractional error ϵ in B_0 the fractional error in the second term on the right side would be $\epsilon\sqrt{2}$, assuming that $\omega_s - \omega_c$ is measured directly but not simultaneously with ω_c. Since for the electron the second term on the right side is only about 0.1% of the first one, the *total* fractional error on the right side is only $\approx 0.001\epsilon\sqrt{2}$, or 1000 times less than that of the field! By measuring $\omega_s - \omega_c$ directly, sideband excitation[14,41] can make another decisive contribution: The electron, when moving at the cyclotron frequency ω_c through an inhomogeneous magnetic rf field at ω_{ad} sees in its rest frame also sidebands at $|\omega_{ad} \pm \omega_c|$. Thus, by choosing $\omega_{ad} + \omega_c = \omega_s$ one can tune a sideband to the spin resonance and induce spin flips. Not even a millimeter wave source is required because the cyclotron motion is excited thermally and the correct ω_{ad} value falls near $2\pi \times 163$ MHz.

However, another serious problem remains: The axial motion through the magnetic bottle field produces an average magnetic field shift proportional to the axial motion energy E_z. Worse, E_z contains a cross term proportional to $z_t z_c$, where z_t and z_c are oscillation amplitudes excited thermally (including zero-point motion) and by the coherent applied drive. This random amplitude cross term, which grows in proportion to the applied detection drive amplitude, broadens the $\omega_s - \omega_c$ and ω_e resonances. For fixed ω_{ad} drive, this broadening reduces the spin-flip rate. The latter effect, namely, the partial suppression of transitions by more frequent continuous state measurement[42,43] made possible by the stronger axial drive, is the toothless ghost of the formidable Zeno no-go theorem of the last section. Moreover, line broadening is easily avoided by alternating periods of spin-flip excitation during which the axial detection drive is turned off with state monitoring periods in which the axial drive necessary for ω_z measurement is on but the spin-flip excitation is off. In the alternating mode, for very strong excitation the probabilities for finding spin-up or spin-down in a monitoring period are 50% each. Thus, on the average in N excitation/monitoring cycles, one can count no more than $N/2$ jumps from one m level to the other. This indicates saturation of the resonance and strong broadening and distortion of the weak signal line shape one is looking for. In the resonance shown in Fig. 5, a reasonable compromise was struck with a maximum count of 10 jumps in 25 cycles. The resonance was obtained making full use of the above discussion (compare also Fig. 6). In the energy level diagram of Fig. 3, a spin flip $(n=0,\ m=-\frac{1}{2}) \rightarrow (n=0,\ m=+\frac{1}{2})$ induced in the above fashion may be viewed as a transition $n=0 \rightarrow 1$ due to thermal radiation followed by a transition $(n=1,\ m=-\frac{1}{2}) \rightarrow (n=0,\ m=+\frac{1}{2})$ induced by the applied rf field at ω_a, and therefore termed a two-photon transition. In accordance with the fact that for the parameter values of the 1984 geonium experiments due to thermal excitation the electron spends on the average about 5 s in the $n=0$, but only 1 s in the $n=1$ states, spin flips $m=-\frac{1}{2} \rightarrow +\frac{1}{2}$ proceed on the average much more slowly than for $m=+\frac{1}{2} \rightarrow -\frac{1}{2}$.

VII. CONCLUSION

Single trapped-ion work that I initiated with my students and associates in the early 1970s has by now yielded important results and opened many new research avenues: From precision measurements of the magnetic moment of the electron, an elementary particle, a new 10 000 times smaller value of its radius has been derived. Extension of these measurements to the positron has produced the most stringent test of matter/antimatter symmetry for a *charged* particle pair. For the first time, quantum measurements have been performed on the same individual atomic particle as often as one pleases and new tests of measurement theory have become possible.[42,43] Zero-point confinement in the lowest quantum levels of traps in one[20] and two[33,34] degrees of freedom of motion has been reported. The largest (by 90%) suppression of spontaneous emission from an atomic particle has been demonstrated. Single atomic ion passive optical frequency standards[20,21,30] promise a reproducibility for unlimited periods that is up to 100 000 times better than the current state of the art. With the growing extension of geonium techniques into the optical region,[4,21] to photon statistics,[44] ion crystal,[45,46] and chaos[47] studies, and to neutral atoms,[48] one may hope a discussion of some of the simple ideas[49] underlying these techniques will be of use to a widening circle of readers.

ACKNOWLEDGMENTS

I should like to thank my colleagues, Fred Palmer and Paul Schwinberg, for reading the manuscript and offering valuable suggestions. The National Science Foundation has supported my research since 1958.

[1] H. Dehmelt, "Radiofrequency spectroscopy of stored ions," Adv. At. Mol. Phys. 3, 55 (1967); 5, 109 (1969).

[2] H. Dehmelt, "Stored-ion spectroscopy," in *Advances in Laser Spectroscopy*, edited by F. T. Arecchi, F. S. Strumia, and H. Walther (Plenum, New York, 1983).

[3] R. S. Van Dyck, Jr., P. B. Schwinberg, and H. G. Dehmelt, "Electron

magnetic moment from geonium spectra: Early experiments and background concepts," Phys. Rev. D **34**, 722 (1986).
[4]H. Dehmelt, "A single atomic particle forever floating at rest in free space," Phys. Scr. T **22**, 102 (1988); see references cited herein.
[5]H. Dehmelt, "New continuous Stern Gerlach effect and a hint of 'the' elementary particle," Z. Phys. D **10**, 127 (1988), and references cited therein.
[6]D. J. Wineland, P. Ekstrom, and H. Dehmelt, "Monoelectron oscillator," Phys. Rev. Lett. **31**, 1279 (1973).
[7]P. B. Schwinberg, R. S. Van Dyck, Jr., and H. G. Dehmelt, "Trapping and thermalization of positrons for geonium spectroscopy," Phys. Lett. A **81**, 119 (1981).
[8]R. S. Van Dyck, Jr., P. B. Schwinberg, and H. G. Dehmelt, "The electron and positron geonium experiments," in *Atomic Physics 9*, edited by R. S. Van Dyck, Jr. and E. N. Fortson (World Scientific, Singapore, 1984), p. 53.
[9]R. S. Van Dyck, Jr., P. Ekstrom, and H. Dehmelt, "Axial, magnetron, cyclotron, and spin-cyclotron beat frequencies measured on single electron almost at rest in free space (geonium)," Nature **262**, 776 (1976).
[10]R. S. Van Dyck, Jr., P. B. Schwinberg, and H. G. Dehmelt, "Electron magnetic moment from geonium spectra," in *New Frontiers in High Energy Physics*, edited by B. Kursunoglu, A. Perlmutter, and L. F. Scott (Plenum, New York, 1978).
[11]H. Dehmelt and P. Ekstrom, "Proposed g-2/$\delta\omega_z$ experiment on single stored electron or positron," Bull. Am. Phys. Soc. **18**, 727 (1973).
[12]H. Dehmelt, "Entropy reduction by motional side band excitation," Nature **262**, 777 (1976).
[13]A. Kastler, "Optical methods of atomic orientation and of magnetic resonance," J. Opt. Soc. Am. **47**, 460 (1957).
[14]F. Walls, "Determination of the anomalous magnetic moment of the electron from measurements made on an electron gas at 80 K using a bolometric technique," Doctoral Thesis, University of Washington, 1970.
[15]R. Van Dyck, Jr., P. Schwinberg, and H. Dehmelt, "New high-precision comparison of electron and positron g factors," Phys. Rev. Lett. **59**, 26 (1987).
[16]T. Kinoshita, "Fine-structure constant derived from quantum electrodynamics," Metrologia **25**, 233 (1988).
[17]S. J. Brodsky, and S. D. Drell, "Anomalous magnetic moment and limits on fermion substructure," Phys. Rev. D **22**, 2236 (1980).
[18]L. Lyons, "An introduction to the possible substructure of quarks and leptons," Prog. Part. Nucl. Phys. **10**, 227 (1983); see references cited herein.
[19]H. Dehmelt, "Triton..., electron..., cosmon...: An infinite regression?," Proc. Natl. Acad. Sci. USA **86**, 8618 (1989).
[20]H. Dehmelt, "Single atomic particle at rest in free space: New value for electron radius," Ann. Phys. (Paris) **10**, 777–795 (1985).
[21]W. Itano, J. Bergquist, and D. Wineland, "Laser spectroscopy of trapped atomic ions," Science **237**, 612 (1987).
[22]H. Dehmelt, "Coherent spectroscopy on a single atomic system at rest in free space III," in *Frequency Standards and Metrology*, edited by A. de Marchi (Springer, New York, 1989), p. 15.
[23]R. Van Dyck, F. Moore, D. Farnham, and P. Schwinberg, "Single proton isolated and resolved in Penning trap," Bull. Am. Phys. Soc. **31**, 974 (1986).
[24]G. Gabrielse *et al.*, "First capture of antiprotons in a Penning trap," Phys. Rev. Lett. **57**, 2504 (1986).
[25]W. Neuhauser, M. Hohenstatt, P. E. Toschek, and H. G. Dehmelt, "Optical-sideband cooling of visible atom cloud confined in parabolic well," Phys. Rev. Lett. **41**, 233 (1978).
[26]W. Neuhauser, M. Hohenstatt, P. E. Toschek, and H. Dehmelt, "Localized visible Ba^+ mono-ion oscillator," Phys. Rev. A **22**, 1137 (1980).
[27]W. Nagourney, "The mono-ion oscillator: An approach to an ideal atomic spectrometer," Comments At. Phys. **XXI**, 321 (1988), and Philip Morrison and Phyllis Morrison, *The Ring of Truth* (Random House, New York, 1987), p. 220.
[28]No individual *neutral* atom has so far been isolated and trapped, though there is great ferment in the field and many of the processes generic to trapped particles previously described for ions (see Ref. 4) are being rediscovered.
[29]W. Nagourney, J. Sandberg, and H. Dehmelt, "Shelved optical electron amplifier: Observation of quantum jumps," Phys. Rev. Lett. **56**, 2797 (1986).
[30]Hans Dehmelt, Nan Yu, and Warren Nagourney, "The 6^1S_0–6^3P_0 transition in thallium isotope ion $(^{204}Tl)^+$: A superior atomic clock," Proc. Natl. Acad. Sci. USA **86**, 3938 (1989), and H. Dehmelt, "Mono-ion oscillator as potential ultimate laser frequency standard," IEEE Trans. Instrum. Meas. **IM-31**, 83 (1982).
[31]J. Bergquist, F. Diedrich, W. Itano, and D. Wineland, "Hg^+ single ion spectroscopy," in *Frequency Standards and Metrology*, edited by A. de Marchi (Springer, New York, 1989).
[32]W. Nagourney, N. Yu, and H. Dehmelt, "Laser spectroscopy on single barium ion using 'shelving,' " in *Frequency Standards and Metrology*, edited by A. de Marchi (Springer, New York, 1989).
[33]F. Diedrich, J. Bergquist, W. Itano, and D. Wineland, "Laser cooling to the zero-point energy of motion," Phys. Rev. Lett. **62**, 403 (1989).
[34]Nan Yu, Hans Dehmelt, and Warren Nagourney, "Trapped individual ion at absolute zero temperature," Proc. Natl. Acad. Sci. USA **86**, 5671 (1989).
[35]H. Dehmelt, "RF-spectroscopy of trapped ions by a selective elimination–collision technique," Bull. Am. Phys. Soc. **7**, 470 (1962).
[36]E. M. Purcell, "Spontaneous emission probabilities at radio frequencies," Phys. Rev. **69**, 681 (1946).
[37]H. Dehmelt, P. Ekstrom, and D. Wineland, "Thermal noise in the monoelectron oscillator," Bull. Am. Phys. Soc. **19**, 572 (1974).
[38]H. Dehmelt (unpublished, 1977).
[39]D. Wineland, "Laser-to-microwave frequency division using synchrotron radiation," J. Appl. Phys. **50**, 2528 (1979).
[40]R. S. Van Dyck, P. Schwinberg, G. Gabrielse, and H. Dehmelt, "Geonium spectra and the finer structure of the electron," Bull. Magn. Res. **4**, 17 (1983).
[41]H. Dehmelt and F. Walls, "Bolometric technique for the rf spectroscopy of stored ions," Phys. Rev. Lett. **21**, 127 (1968), and D. J. Wineland and H. G. Dehmelt, "Principles of the stored ion calorimeter," J. Appl. Phys. **46**, 919 (1975).
[42]H. Dehmelt, "Continuous Stern Gerlach effect: Noise and the measurement process," Proc. Natl. Acad. Sci. USA **83**, 3074 (1986).
[43]W. M. Itano, D. J. Heinzen, J. J. Bollinger, S. L. Gilbert, and D. J. Wineland, "Tests of quantum mechanics with laser-cooled ions," Bull. Am. Phys. Soc. **34**, 1688 (1989).
[44]F. Diedrich and H. Walther, "Nonclassical radiation of a single stored ion," Phys. Rev. Lett. **58**, 203 (1987).
[45]F. Diedrich, E. Peik, J. Chen, W. Quint, and H. Walther, "Observation of phase transitions of stored laser-cooled ions," Phys. Rev. Lett. **59**, 2931 (1987).
[46]T. Sauter, H. Gilhaus, I. Siemens, R. Blatt, W. Neuhauser, and P. Toschek, "On the photo-dynamics of single ions in a trap," Z. Phys. D **10**, 153 (1988).
[47]J. Hoffnagle, R. DeVoe, L. Reyna, and R. Brewer, "Order–chaos transition of two trapped ions," Phys. Rev. Lett. **61**, 255 (1988).
[48]D. Pritchard, K. Helmerson, and A. Martin, "Atom traps," in *Atomic Physics 11*, edited by S. Haroche, J. C. Gay, and G. Grynberg (World Scientific, Singapore, 1989).
[49]The validity of the ideas employed in carrying out the original geonium experiments has later been confirmed in L. S. Brown and G. Gabrielse, "Geonium theory," Rev. Mod. Phys. **58**, 233 (1986). While the *mechanism* for producing spin flips by means of an axial rf *electric* field at ν_a as proposed by Dehmelt and Ekstrom in 1973 was ineffective, this elegantly simple experimental scheme (see Refs. 3 and 8) works very well indeed, by a different mechanism, and was the only one used in the geonium experiments until 1982.